

Post-B3LYP Functionals Do Not Improve the Description of Magnetic Coupling in Cu(II) Dinuclear Complexes

DOI:

[10.1021/acs.jpca.7b12663](https://doi.org/10.1021/acs.jpca.7b12663)

Document Version

Accepted author manuscript

[Link to publication record in Manchester Research Explorer](#)

Citation for published version (APA):

Costa, R., Reta, D., Moreira, I. D. P. R., & Illas, F. (2018). Post-B3LYP Functionals Do Not Improve the Description of Magnetic Coupling in Cu(II) Dinuclear Complexes. *Journal of Physical Chemistry A*. <https://doi.org/10.1021/acs.jpca.7b12663>

Published in:

Journal of Physical Chemistry A

Citing this paper

Please note that where the full-text provided on Manchester Research Explorer is the Author Accepted Manuscript or Proof version this may differ from the final Published version. If citing, it is advised that you check and use the publisher's definitive version.

General rights

Copyright and moral rights for the publications made accessible in the Research Explorer are retained by the authors and/or other copyright owners and it is a condition of accessing publications that users recognise and abide by the legal requirements associated with these rights.

Takedown policy

If you believe that this document breaches copyright please refer to the University of Manchester's Takedown Procedures [<http://man.ac.uk/04Y6Bo>] or contact uml.scholarlycommunications@manchester.ac.uk providing relevant details, so we can investigate your claim.



Post-B3LYP Functionals Do Not Improve the Description of Magnetic Coupling in Cu(II) Dinuclear Complexes

Ramon Costa, Daniel Reta, Ibério de P.R. Moreira, and Francesc Illas

J. Phys. Chem. A, **Just Accepted Manuscript** • DOI: 10.1021/acs.jpca.7b12663 • Publication Date (Web): 06 Mar 2018

Downloaded from <http://pubs.acs.org> on March 12, 2018

Just Accepted

“Just Accepted” manuscripts have been peer-reviewed and accepted for publication. They are posted online prior to technical editing, formatting for publication and author proofing. The American Chemical Society provides “Just Accepted” as a service to the research community to expedite the dissemination of scientific material as soon as possible after acceptance. “Just Accepted” manuscripts appear in full in PDF format accompanied by an HTML abstract. “Just Accepted” manuscripts have been fully peer reviewed, but should not be considered the official version of record. They are citable by the Digital Object Identifier (DOI®). “Just Accepted” is an optional service offered to authors. Therefore, the “Just Accepted” Web site may not include all articles that will be published in the journal. After a manuscript is technically edited and formatted, it will be removed from the “Just Accepted” Web site and published as an ASAP article. Note that technical editing may introduce minor changes to the manuscript text and/or graphics which could affect content, and all legal disclaimers and ethical guidelines that apply to the journal pertain. ACS cannot be held responsible for errors or consequences arising from the use of information contained in these “Just Accepted” manuscripts.



Post-B3LYP Functionals Do Not Improve the Description of Magnetic Coupling in Cu(II) Dinuclear Complexes

Ramon Costa,^{1,2} Daniel Reta,³ Ibério de P. R. Moreira,^{1,4} and Francesc Illas^{*,1,4}

¹*Institut de Química Teòrica i Computacional (IQTCUB),*

Universitat de Barcelona, C/ Martí i Franquès 1, E-08028 Barcelona, Spain.

²*Departament de Química Inorgànica i Orgànica, Universitat de Barcelona,*

C/ Martí i Franquès 1, E-08028 Barcelona, Spain.

³*School of Chemistry, The University of Manchester,*

Oxford Road, Manchester, M13 9PL, United Kingdom

⁴*Departament de Ciència dels Materials i Química Física, Universitat de*

Barcelona, C/ Martí i Franquès 1, E-08028 Barcelona, Spain.

Abstract

The accuracy of post-B3LYP functionals is analyzed using an open shell database of Cu(II) dinuclear complexes with well defined experimental values of the magnetic coupling constants. This database provide a sound open shell training set to be used to improve the fitting schemes in defining new functionals or when reparametrizing the existing ones. For a large set of representative hybrid exchange-correlation functionals, it is shown that the overall description of moderate to strong antiferromagnetic interactions is significantly more accurate than the description of ferromagnetic or weakly antiferromagnetic interactions. In the case of global hybrids, the most reliable ones have 25-40% Fock exchange with SOGGA and PBE0 being the most reliable and M06 the exception. For range corrected hybrids, the long range corrected CAM-B3LYP and ω B97XD provide acceptable results and M11 is comparable but more erratic. It is concluded that the reliability of the calculated values is system and range dependent and this fact introduces a serious warning on the blind use of a single functional to predict magnetic coupling constants. Hence, in order to extract acceptable magnetostructural correlations, a “standardization” of the method to be used is advised to choose the optimal functional.

*Corresponding author: francesc.illas@ub.edu

1. Introduction.

One of the goals of quantum chemistry is solving the time-independent Schrödinger equation for n electrons moving in an electric field generated by N (fixed) nuclei.^{1,2} The solution provides the energy and the wave functions of the quantum mechanical states of this system for different nuclear configurations and hence provides a general scheme to obtain equilibrium geometries and properties of the ground state, as well as of excited states. In practice, one focuses on obtaining approximate wave functions $\Psi_i(\mathbf{r}_1s_1, \dots, \mathbf{r}_ns_n)$ that explicitly depend on the $3n$ spatial coordinates ($4n$ including spin) of all electrons in the system. From the wave functions one can derive an explicit form of the energy functional in terms of the one- and two-electron density matrices respectively leading to $E[\gamma_1(\mathbf{r}_1; \mathbf{r}_1'), \gamma_2(\mathbf{r}_1, \mathbf{r}_2; \mathbf{r}_1', \mathbf{r}_2')]$.^{1,2,3} However, the exact solution becomes unattainable except in a finite basis— leading to the well known full configuration interaction expansion— and for a very limited number of electrons only. Therefore, simplified wave functions are normally used as in the case of the Hartree-Fock method, a mean field approximation neglecting instantaneous electron-electron interactions usually referred to as electron correlation effects. Going beyond this approximation becomes soon intractable except for small gas phase molecules thus limiting its application for general purposes.

Density functional theory (DFT) provides an alternative approach to describe the energy E of the electronic ground state of the system of n electrons and N nuclei in terms solely of the electronic density distribution $\rho(\mathbf{r})$ that explicitly depends on 3 coordinates: the trace of the $\gamma_1(\mathbf{r}_1; \mathbf{r}_1')$ one electron density matrix. This theory is based on the Hohenberg and Kohn theorems.⁴ The first theorem states that for a system of n electrons and N nuclei in a non-degenerate ground state, the ground state density determines the external potential $V(\mathbf{r})$ uniquely (except perhaps to an additive constant), and since it also determines n by integration, it determines the full Hamiltonian and (through a big jump in an unknown direction other than solving the Schrödinger equation) all the properties of the system. An important corollary is that the energy of the ground state, E , can be obtained from the exact electron density by means of a universal functional $E[\rho(\mathbf{r})]$ of the electron density $\rho(\mathbf{r})$ only. The second theorem states that for any density other than the exact one, the energy obtained from this exact functional is higher than the one corresponding to the exact density which opens a way for practical applications.

1
2
3 The theorems do not provide the form of this universal, exact, yet unknown,
4 functional and a large theoretical effort has been devoted to justify some of its
5 properties and variational behavior since its introduction in 1964. Soon after, Kohn
6 and Sham⁵ introduced a reference non interacting system to provide a formal structure
7 of the terms in the $E[\rho(\mathbf{r})]$ functional. Using a single Slater determinant to describe
8 $\rho(\mathbf{r})$, the variational procedure leads to a set of one electron equations with the same
9 structure to the Hartree-Fock ones in which the still unknown universal exchange-
10 correlation energy functional, $E_{xc}[\rho(\mathbf{r})]$, includes all the complicated electron-electron
11 correlation effects as well as the missing kinetic energy terms.⁶

12
13
14 During the last two decades, density functional theory (DFT) has become a
15 fundamental tool for modern quantum-chemical modeling of molecules and materials
16 in many different areas of physics, chemistry and biochemistry.⁷ Large efforts have
17 been developed to produce many different approximations to the unknown $E_{xc}[\rho(\mathbf{r})]$
18 functional in order to obtain accurate energies and electron densities of molecular and
19 solid state systems and, hence, to attain a useful and reliable description of their
20 physical and chemical properties. To this end, several benchmarks, including
21 thermochemistry and energy barriers for chemical reactions, have been selected to
22 optimize the functional forms of the exchange-correlation potentials in the Kohn-Sham
23 approximation.⁵ These benchmarks provide experimentally well-defined values which
24 are taken as reference to test functional forms derived from different strategies.

25
26
27 Despite the improvement of the accuracy in describing formation energies of
28 atoms and molecules, bonding energies, molecular and crystal structures, as well as
29 other properties, Perdew and collaborators⁸ pointed out recently that the increasing
30 accuracy attained by post-B3LYP functionals in describing the energy of an electronic
31 system does not necessarily imply a better description of the electron density of the
32 system. For atomic systems, these authors show that even if overparameterized
33 exchange-correlation functionals proposed in the past few years show improved
34 accuracy for the calculated energy, the corresponding densities do not get closer to the
35 exact ones.⁸ This tendency is more evident for the functionals proposed since the early
36 2000s and the authors associate this drawback to the extensive use of unconstrained
37 functionals that rely on the flexibility of empirical fitting by ignoring the known
38 physical constraints to construct the energy functional. Nevertheless, this view is not
39 universally accepted and subject of some controversy.⁹⁻¹¹

1
2
3 An important remark regarding most of the recently proposed density
4 functionals is that these focus essentially in thermochemistry and pay little attention to
5 other properties that can be experimentally measured and directly determined by the
6 low energy spectrum of the system. This is precisely the case of magnetic coupling (J)
7 in diradicals and some inorganic dinuclear complexes, determined by the energy
8 difference between electronic states with different total spin. Following previous
9 work^{12,13} where a series of functionals were tested against a well defined database of
10 open shell systems, we extend our study to analyze the reliability of functionals
11 derived after the very successful and broadly used B3LYP one. In the following we
12 will refer to these functionals as post-B3LYP and will focus on the magnitude of the
13 magnetic coupling constants of a family of dinuclear Cu(II) complexes with a variety
14 of bridging ligands ranging from strong antiferromagnetic to strong ferromagnetic
15 coupling constants. This allows us to establish an “open shell training set” for the
16 testing and calibration newly designed density functionals. The close connection
17 between the calculated J values and the degree of electron delocalization provides
18 additional information to assess the overall performance of a given functional. In this
19 sense, we will advise that a more accurate description of J values along this open shell
20 training set is an indication of an improved description of the spin density distribution
21 as well. We argue that the relevance of this open shell training set goes beyond the
22 particular case of Cu(II) complexes and should be included in the benchmarks used to
23 analyze the performance of new functionals.
24
25
26
27
28
29
30
31
32
33
34
35
36

37 This paper is organized as follows: in Sec. 2 we provide an account of the
38 different improvement paths in developing the DFT functionals up to now. Next we
39 describe in Sec. 3 the molecular compounds with well-defined crystal structure and
40 experimentally known magnetic coupling to establish an open shell training set. In
41 Sec. 4 we describe the computational details and the scheme used to obtain the
42 suitable energy difference and in Sec. 5 we describe the J values predicted by the
43 different functionals in order to analyze their reliability in describing this relevant
44 molecular property. Finally, in Sec. 6 we summarize our remarks and conclusions.
45
46
47
48
49

50 **2.- The open shell database of Cu(II) dinuclear compounds**

51
52 In this section we describe an enlarged set of molecular Cu(II) magnetic
53 systems introduced in previous works^{12,13} as a reference open shell training set to
54
55
56
57
58
59
60

1
2
3 systematically investigate the performance of the post-B3LYP exchange-correlation
4 functionals to predict magnetic coupling constants.
5

6 The Cu(II) dinuclear complexes have been selected in order to minimize ZFS
7 effects, the availability of well characterized molecular crystal structures with a
8 moderate number of atoms, and the diversity of bridging ligands and a wide range of
9 experimentally determined magnetic coupling constants. In order to avoid mixing
10 structural and electronic effects, the crystallographic structures for which the magnetic
11 parameters have been measured have been used without further optimization, except
12 for a few cases where some hydrogen atoms belonging to terminal ligands (not
13 affecting the bridging ones) were not defined: in these cases partial optimizations
14 using B3LYP functional on the triplet states have been used to locate them in
15 approximate positions. To facilitate the calculations of compounds containing
16 ferrocenecarboxylato bridges, these ligands have been replaced by formiato groups, as
17 the magnetic interaction is exclusively mediated by the carboxylate group.
18

19 The selected list of dinuclear Cu(II) complexes covers a broad range of
20 exchange coupling constant J values, ranging from strong antiferromagnetic coupling
21 (singlet-triplet gap of -400 cm^{-1}) to strong ferromagnetic (up to 230 cm^{-1} gap). They
22 contain a wide diversity of bridging ligands (the ones responsible of the magnetic
23 exchange) including water, hydroxo, O- and O,O-carboxylates, oxalate derivatives,
24 and 1,1-azido. In order to identify the selected compounds the standard abbreviations
25 used as REFCODEs in the Cambridge Structural Database System¹⁴ have been used.
26 The details on the molecular structure and properties of some of BISDOW,¹⁵
27 CUAQAC02,¹⁶ CAVXUS,¹⁷ XAMBUI,¹⁸ and YAFZOU¹⁹ have been discussed
28 previously as a reference open shell database by some of us. Here we provide a short
29 description of the main features of the additional complexes considered in this work,
30 namely QAQVIP, PATFOG, JEJCIK and LIZVOF.
31

32 QAQVIP²⁰ consists of well separated dinuclear cations with two
33 pentacoordinated Cu(II) atoms each having a chelating bidentate 2,2'-bipyridine
34 terminal ligand and sharing three bridging ligands (three benzoates, two of them acting
35 as bidentate and one as O,O-monodentate). One of the Cu(II) ions is in a mainly
36 square-pyramidal environment where the monodentate bridging benzoate lies in the
37 apical position. The other metal has a trigonal-bipyramidal pentacoordination where
38 the monodentate bridging benzoate lies in one of the equatorial positions. In this way,
39 it is expected that the main interaction between the magnetic orbitals occurs through
40
41
42
43
44

1
2
3 the two bidentate *O,O'*-carboxylato bridges. The monodentate bridge does not
4 participate in the superexchange interactions thus avoiding countercomplementary
5 effects through this ligand, so only the antiferromagnetic pathways through both
6 bidentate carboxylates remain active.
7
8

9 The PATFOG cation²¹ consists of a trimetallic complex with a dinuclear
10 copper(II) core where the Cu(II) ions are bridged by one hydroxo and one μ -*O,O'*-
11 ferrocenecarboxylate anions. Each copper atom is also bound to one terminal bidentate
12 *N,N,N',N'*-tetramethylethylenediamine (tmen, Me4en) ligand in such a way that the
13 [CuN₂O₃] chromophores define the basal planes of a square-pyramidal coordination.
14 The apical positions are occupied by different oxygen atoms of one of the perchlorate
15 anions, which in fact acts as a third *O,O'* bridge with Cu-O distances longer than 2.4
16 Å, so indicating a 4+1 coordination. Another relevant structural feature of this dimeric
17 cation is the existence of a hydrogen bond between the bridging hydroxo group and
18 one oxygen atom of the other perchlorate anion. The ferrocenyl moiety seems that
19 does not affect the magnetic properties of the system, which exchange is exclusively
20 mediated by its carboxylate group, so to facilitate our calculations it has been replaced
21 by a formiato group.
22
23
24
25
26
27
28
29

30 JEJCIK contains a dinuclear cation²² consisting of a triply bridged pair of five-
31 coordinate copper atoms. Both are in square-planar environments sharing one basal
32 edge and the apical positions. A water molecule acts as the apical bridge whereas a
33 μ -hydroxo and a μ -*O,O'*-acetato are the basal bridging ligands in such a way that the
34 acetato end of the shared edge acts also as a separator. As expected, the apical Cu-O
35 distances are noticeably longer than basal bond distances. The Cu atoms are only
36 0.092 and 0.137 Å out of the basal planes, which form a 61.9 dihedral angle. The Cu-
37 O(H)-Cu bridging angle is 103.8°, a relatively small value that may be contributing to
38 the observed ferromagnetism. The cations form infinite chains as a result of H-
39 bonding interactions with one of the perchlorate anions connecting the OH- hydrogen
40 atom of one cation and one hydrogen atom of the apical water molecule of an adjacent
41 cation. The weak intermolecular antiferromagnetic interactions observed in the
42 measures at low temperature²² are attributed to these contacts.
43
44
45
46
47
48
49
50

51 LIZVOF²³ consists of well-isolated centrosymmetric dinuclear units in which
52 the copper(II) atoms are bridged by two azido ions in end-on conformation. The Cu(II)
53 ions present 4(square-planar) + 1 + 1 coordination, where the nitrogen donors of the 4-
54 ethylpyridine terminal ligands and the bridging nitrogen atoms of each azido anion
55
56
57
58
59
60

1
2
3 form the nearly planar $[\text{N}_2\text{Cu}(\mu_{1,1}\text{-N}_3)_2\text{CuN}_2]^{2+}$ core of the complex. Two $\mu\text{-O,O'}$ -
4 nitrate ions are over and under the above mentioned plane, acting also as weakly
5 bridging ligands and completing the 4 + 1 + 1 coordination around the copper(II)
6 atoms. The four atoms of the $[\text{Cu}_2(\text{N-azido})_2]$ central square ring of the core are in a
7 plane with Cu-N-Cu angles of 98.3° and the azido groups form an angle of $31.3(2)^\circ$
8 with it. The intradimer Cu-Cu distance is 3.024 Å.
9

10
11
12 References and experimental values of the systems considered in this open
13 shell training set are summarized in Table 1 whereas a schematic representation of the
14 atomic structures of the moieties studied in the present work are displayed in Figure 1.
15 Note that counterions are explicitly included in the calculations when the distance to
16 the metal atom is smaller than 2.5 Å. More distant bulky counterions have negligible
17 polarization effect on the central dimeric magnetic unit and are neglected.
18
19
20
21

22 23 **3. Computational details.**

24
25 Selected post-B3LYP DFT methods have been used to obtain the appropriate
26 energy values to be used in the corresponding mapping described below. In all cases,
27 the calculations were carried out within the spin-polarized (unrestricted) formalism
28 based on a single determinant and both high-spin and broken symmetry (BS) solutions
29 were considered.
30
31
32

33 A number of representative hybrid exchange-correlation potentials have been
34 used to explore the reliability of post-B3LYP functionals in describing the magnitude
35 of the magnetic coupling constants of the family of Cu(II) dinuclear compounds
36 described above. In addition to the standard B3LYP^{24,25} (20% HF), PBE0^{26,27} (25%
37 HF) and BHandHLYP²⁸ (50% HF) global hybrid functionals, we used a series of
38 hybrid functionals developed during the last fifteen years in order to analyze the
39 performance of some additional ones and to explore the effect of range separation of
40 the Fock exchange in the functionals that have been accepted to have a large impact in
41 electron localization. However, it has also been suggested that the remaining part of
42 the exchange-correlation functional also plays a significant role in this aspect (see for
43 instance the performance of M06-L in Ref. 12) and here we will also explore this
44 effect including several functionals developed by the Truhlar's group. To this end we
45 have selected the following DFT functionals:
46
47
48
49
50
51
52
53

- 54 a) Full range hybrid functionals or global hybrids: TPSSh (10.0 % HF)
55 proposed by Tao et al.^{29,30}; X3LYP (21.8 % HF) proposed by Xu and
56
57

1
2
3 Goddard,³¹ APFD (22.95 % HF) of Austin et al.³²; the M06 (27.0 % HF), M06-
4 2X (54.0 % HF)³³ and M06-HF (100.0 % HF)^{34,35} family of meta-GGA hybrid
5 functionals proposed by Zhao and Truhlar as well as their local version M06-L
6 (0.0 % HF)³⁶ for completion since it is one of the most reliable local functional
7 available; and the SOGGA11X (40.15 % HF) proposed by Peverati and
8 Truhlar.³⁷

9
10
11 b) Range separation corrected hybrid functionals: (SR % HF - LR % HF)

12 b.1) Short range corrected: HSE06 (25.0 % - 0 %) proposed by Heyd, Scuseria
13 and Ernzerhof³⁸ and the MN12SX (25.0 % - 0 %) and N12SX (25.0 % - 0 %)
14 proposed by Peverati and Truhlar.³⁹

15 b.2) Long range corrected: ω B97XD (0 % - 100.0 %) of Chai and Head-
16 Gordon,⁴⁰ CAM-B3LYP (0 % - 100.0 %) by Yanai, Tew, and Handy,⁴¹ LC-
17 ω PBE (0 % - 100.0 %) implemented by Vydrov et al.^{42,43}

18 b.3) the short and long range corrected functional M11 (42.8 % - 100 %) by
19 Peverati and Truhlar.⁴⁴

20
21 For each one of the different systems described above, we have computed the
22 magnetic coupling constant with the use of both the broken symmetry and the triplet
23 solutions in the unrestricted (spin-polarized) formalism of a wide variety of state of the
24 art exchange-correlation DFT hybrid functionals. Clearly, in this type of formalism,
25 the spin symmetry is not guaranteed,⁴⁵ although approximate triplet (*T*) states have
26 been obtained from the unrestricted Kohn-Sham formalism using a single Slater
27 determinant with two unpaired electrons (i.e., $S_z = 1$), whereas to estimate the energy
28 of the open shell singlet state we have relied on the broken-symmetry (*BS*) approach
29 imposing $S_z = 0$. In this way, the singlet-triplet gap energy has been obtained on the
30 basis of the Heisenberg spin model Hamiltonian
31
32
33
34
35
36
37
38
39
40
41
42
43
44

$$H = -J \mathbf{S}_1 \cdot \mathbf{S}_2$$

45
46
47
48 and using the appropriate mapping based in the expectation value of the Heisenberg
49 Hamiltonian derived from the single determinant approximation for the *T* and *BS*
50 states leads to the approximate relation:
51
52
53

$$J = 2 [E(BS) - E(T)]$$

1
2
3 where $E(BS)$ is the energy of the broken-symmetry state and $E(T)$ is the energy of the
4 spin unrestricted approximation to the triplet state.
5

6 All DFT calculations were carried out using suitable Gaussian Type Orbitals
7 (GTO) basis sets. For non-metal atoms, the all-electron standard 6-31G(d) basis set
8 has been selected. For the Cu atoms, we used all-electron rather large standard basis
9 set GTO 6-3111+G extended with an f-function (exponent(f) = 0.528). The basis sets
10 chosen were the same as in previous works.^{46,47} Clearly, relativistic effects are not
11 accounted for and one may wonder which effect these may have on the calculated
12 magnetic coupling constants. This issue has been addressed in previous work for
13 embedded cluster models of superconducting cuprate parent compounds where the
14 magnetic coupling constant is defined in a similar way as the energy difference
15 between singlet and triplet states.⁴⁸ Using different types of wave function based
16 methods it was found that the average effect of the basis set, of the description of the
17 Cu core electrons (all electron versus relativistic effective core potentials) and of the
18 electronic structure methods (CASPT2 versus DDCI) was roughly 5%. In any case, the
19 influence of relativistic effects will be identical for all the density functionals
20 considered and, at most, calculated results would have to be equally corrected by a
21 small systematic amount.
22
23
24
25
26
27
28
29
30
31

32 All calculations were performed on the crystallographic structures of the
33 isolated bimetallic complexes (cationic or neutral) in vacuo. This choice prevents
34 mixing structural and electronic effects and avoids introducing inaccuracies in the
35 magnetic coupling constants arising from errors in the structure optimization. The full
36 set of DFT based calculations have been carried out using the Gaussian09 suite of
37 programs.⁴⁹
38
39
40
41

42 **4. Results and discussion.**

43

44 The whole set of calculated J values for the systems studied in this work are
45 summarized in Table 2. Compounds are listed left to right ordered from most
46 antiferromagnetic to most ferromagnetic, and up to down in two different sets to
47 separate global from range separated hybrids. To facilitate the analysis, experimental
48 values are presented in a row between results for the two types of functionals. In each
49 group, the functionals are ordered according to increasing percentage of Fock
50 exchange on the DFT functional. In the lower subset of range separated hybrids, the
51 PBE0 results are included as a reference since most of the functionals are
52
53
54
55
56
57
58
59
60

1
2
3 modifications of this one. A more graphical picture is provided by Figure 2 where
4 experimental values correspond to the continuous line. This figure clearly show that
5 for each compound a large dispersion is found regarding predictions of the different
6 DFT based methods.
7
8

9 To help to classify the performance of each of the explored methods a
10 statistical analysis has been carried out with results summarized in Tables 3 and 4
11 reporting results in terms of relative error values of J_{calc} relative to J_{exp} (in cm^{-1}) using
12 global hybrid DFT functionals and range separated hybrid DFT functionals,
13 respectively. In a similar way, Tables 5 and 6 summarize the corresponding mean
14 absolute error (MAE) values. Finally, a , b , and R values for linear regressions between
15 J_{calc} and J_{exp} (in cm^{-1}) for the full set of compounds and for the FM and AF subsets
16 separately are reported in Table S1 in the supporting information.
17
18

19 For the cases in the present open shell database, all functionals converge and
20 give ferro- (F) and antiferromagnetic (AF) solutions with ground state compatible with
21 experiment and with the calculated spin density at the metal centers. Nevertheless, the
22 calculated J values show a large dispersion and, in some cases, display large
23 deviations with respect to the experiment as can be seen in Tables 3 and 4. The effect
24 of the functional is clearly seen in Figure 3 where the deviation from experiment for
25 the whole database is displayed for each DFT based method. This figure shows that
26 the dispersion is huge for functionals not including Fock exchange such as M06-L or
27 just a small amount (10% in TPSSh) and is progressively reduced with increasing the
28 amount of Fock exchange as in BHandHLYP or M06-2X although not reaching an
29 acceptable accuracy. The importance of the Fock exchange indicates that all explored
30 functionals have difficulties in providing a balanced description of non dynamical and
31 dynamical correlation.
32
33

34 Going in more detail in Tables 3 and 4 one can readily observe that for
35 PATFOG and JEJCIK, with experimentally determined small ferromagnetic
36 couplings, most functionals give relative errors larger than 100 %; interestingly M06-
37 2X and N12SX methods predict acceptable J values for PATFOG but not for JEJCIK.
38 In the case of JEJCIK one can attribute the error to difficulties in the experimental
39 measurement which is based in the use of the the Bleaney-Bowers equation which is
40 only reliable for $T > 50\text{K}$.²² Nevertheless, the fact that the same problem is encountered
41 in PATFOG indicates that these functionals have difficulties in describing
42 ferromagnetic interactions. This behavior can be also observed in view of the mean
43
44
45
46
47
48
49
50
51
52
53
54
55
56
57

1
2
3 absolute error (MAE) for the analyzed functionals reported in Tables 5 and 6. For the
4 full set of complexes under study, ω B97XD and CAM-B3LYP exhibit the smallest
5 MAE values although with large errors for the ferromagnetic systems whereas N12SX
6 and M06-2X provide a more balanced description of ferro- and antiferromagnetic
7 compounds. Nevertheless, the N12SX performs much better for AF compounds,
8 whereas M06-2X gives best results for the ferromagnetic (FM) ones including a fair
9 description of systems with small J values, either FM or AF. To better analyze this
10 trend, columns 2 and 3 of Tables 5 and 6 consider the relative deviation and MAE
11 values for AF and FM systems separately. In addition, Tables 3 and 4 show that
12 ω B97XD and CAM-B3LYP perform very well for AF coupling constants with rather
13 small relative deviation for BISDOW, CUAQAC02, QAQVIP and larger but
14 acceptable (25%) for CAVXUS. A closer look shows for CAVXUS this corresponds
15 to absolute errors of less than 5 cm^{-1} . For the FM set, the M06-2X functional gives by
16 far the best mean results even if the relative errors seem important. However, Table 2
17 makes it clear that the worst cases are XAMBUI with an absolute error of less than 2
18 cm^{-1} and JEJCIK with an overestimation of 27 cm^{-1} . This particular compounds shows
19 how severe the problem is in compounds with small J requiring to treat non-dynamical
20 and dynamical correlation on equal foot which is a challenge for DFT based methods.
21
22
23
24
25
26
27
28
29
30
31

32 Finally, we comment on the linear regressions for each individual functional
33 data set (see Table S1) with respect to the experimental values. The analysis of these
34 fits give the best overall correlation coefficients for X3LYP, APFD and PBE0
35 functionals, although their slopes are strongly deviated from unity, thus indicating
36 different behaviors for FM and AF couplings. Interestingly, a slope closer to 1
37 corresponds to SOGGA method, which shows a constant deviation of $+45 \text{ cm}^{-1}$.
38 Unfortunately, attempts to take advantage of this correct trend fail for small couplings.
39 The ω B97XD functional shows a good compromise between a satisfactory prediction
40 of AF coupling constants and a linear correlation with experimental values and
41 concomitant slope close to unity although it tends to overestimate the FM couplings.
42
43
44
45
46
47

48 A final observation concerns the calculated spin densities in the metal centers.
49 For selected compounds this is reported in Table S2 of the supporting information. All
50 functionals providing quite accurate numerical J values, especially those in the range
51 separated family, tend to predict similar values of the spin density as well whereas this
52 trend breaks down for functionals performing poorly. This seems to provide an
53
54
55
56
57
58
59
60

1
2
3 indication that it is well possible to obtain a quite good estimate of the magnetic
4 coupling and of the electron density as would be expected for the exact functional.⁸
5

6 **5. Conclusions**

7
8 A general observation regarding the complete set of systems studied is that
9 predicted magnetic coupling constants in dinuclear Cu(II) complexes are system
10 dependent and sensitive to the magnitude and sign of the dominant exchange
11 mechanism.
12

13
14 As a general trend it is observed that MAE errors for range-separated
15 functionals are lower than for global hybrids. The ω B97XD and CAM-B3LYP, both
16 long range corrected with 100 % Fock exchange, show a very good performance in
17 reproducing the experimental values for AF couplings. On the contrary, M11 and
18 N12SX provide slightly better estimates for FM couplings with noticeable accuracy in
19 the description of AF compounds as well.
20
21
22
23

24
25 Regarding global hybrids, the most reliable results are obtained with those
26 having 25-40% Fock exchange with SOGGA and PBE0 being the most reliable and
27 M06 the exception. For range corrected hybrids, the long range corrected CAM-
28 B3LYP and ω B97XD provide acceptable results and M11 is comparable but more
29 erratic. We are confident that this conclusion will hold for other magnetic systems as
30 well.
31
32
33

34
35 The present results consistently show that the description of moderate to strong
36 antiferromagnetic interactions is significantly more accurate than the description of
37 ferromagnetic or weakly antiferromagnetic interactions. In general, the description of
38 FM systems appears to be much less reliable than that observed for systems with AF
39 coupling. Moreover, in FM systems a large dispersion of values is obtained for
40 functionals with similar amount of Fock exchange. Clearly, the description of
41 ferromagnetic coupling constants is not satisfactorily reproduced with any of the
42 functionals explored M06-2X (54 % Fock) and BHandHLYP (50 % Fock) being those
43 that provide acceptable estimates but with significant erratic deviations especially for
44 moderate to strong positive couplings, and its use is recommend to have a guessing
45 approach only. Taking into account the present results, the most reliable functionals
46 for moderate to strong AF coupled systems are PBE0 and APFD global hybrids and
47 ω B97XD and CAM-B3LYP long range corrected hybrids. MN12X short range
48 corrected hybrid provides significant correlation values, especially for FM systems.
49
50
51
52
53
54
55
56
57

1
2
3 An important dispersion of results is also observed with respect to the
4 experimental values along the set of systems. None of the studied functionals provide
5 an overall balanced description of the singlet triplet energy gap for all the systems.
6 However, from the J_{calc} vs. J_{expt} linear regressions, those providing a value of the
7 independent term closest to zero should be the most reliable for magnetostructural
8 correlations. However, it should be emphasized that a and b values of linear
9 regressions strongly depend on the range considered. This is a clear indication that the
10 reliability of the calculated values is system and range dependent and introduces a
11 serious warning on the blind use of a single functional to predict magnetic coupling
12 constants. Hence, it is advised performing a “standardization” of the method to be
13 used against a well defined benchmark set of systems with known values of J with a
14 similar structure and J values. This will allow the possibility of extracting acceptable
15 magnetostructural correlations for a set of similar compounds using the optimal
16 functional.

17
18
19 In conclusion, the present open shell database of Cu(II) dinuclear complexes
20 provides a sound open shell training set to be used to improve the fitting schemes in
21 defining new functionals or when reparametrizing the existing ones. The present result
22 are likely to be relevant for other properties such as chemical reactivity where
23 intermediates and transition states often exhibit multireference character and well
24 defined experimental data is not always directly available.

25 26 27 28 29 30 31 32 33 34 35 36 37 **Acknowledgments**

38
39 This research was supported by the Spanish MINECO, the Agencia Estatal de
40 Investigación (AEI) and Fondo Europeo de Desarrollo Regional (FEDER) through
41 projects CTQ2015-64618-R and CTQ2016-76423-P grants and, in part, by Generalitat
42 de Catalunya (grants 2017SGR13, 2017SGR348 and XRQTC). FI acknowledges
43 additional support from the 2015 ICREA Academia Award for Excellence in
44 University Research.
45
46
47
48
49
50
51
52
53
54
55
56
57
58
59
60

ASSOCIATED CONTENT**Supporting Information**

The Supporting Information is available free of charge on the ACS Publications website at DOI:

Table S1. *a*, *b*, and *R* values for linear regressions between J_{calc} and J_{exp} (in cm^{-1}) for the full set of compounds and for the FM and AF subsets separately

Table S2. Spin densities on Cu(II) centres from Mulliken population analysis for selected systems. Positive (negative) values represent α (β) spin densities. A single absolute value is provided except in the cases where a significant difference between the two magnetic centers is observed.

AUTHOR INFORMATION**Corresponding Author**

* E-mail: francesc.illas@ub.edu

Notes

The authors declare no competing financial interest.

Table 1. Cambridge Crystallographic Data Base (CCDB) names, experimental J values (in cm^{-1}) and reference of the molecular systems studied.

Complex	CCDB Name	J	Reference
1	BISDOW	-382.00	15
2	CUAQAC02	-286.00	16
3	QAQVIP	-39.70	20
4	CAVXUS	-19.00	17
5	XAMBUI	2.50	18
6	PATFOG	29.00	21
7	JEJCIK	38.00	22
8	YAFZOU	111.00	19
9	LIZVOF	230.00	23

Table 2. Calculated DFT J values (in cm^{-1}) of the molecular systems studied using the broken symmetry approach for global and range separated functionals.

HF %	Functional	bisdow	cuaqac02	qaqvip	cavxus	xambui	patfog	jejcik	yafzou	lizvof
0	M06-L	-1316.0	-752.0	-138.7	-25.0	23.0	119.7	273.6	334.0	139.3
10	TPSSh	-918.9	-586.8	-105.3	-26.9	8.8	52.4	173.4	193.4	226.9
20	B3LYP	-633.9	-429.4	-70.9	-21.2	3.9	74.7	163.4	193.6	304.2
21.8	X3LYP	-578.0	-398.4	-63.4	-19.2	3.5	74.7	157.4	186.7	322.3
22.945	APFD	-546.5	-378.8	-58.7	-18.3	3.4	74.1	151.2	179.7	345.0
25	PBE0	-492.0	-346.0	-51.6	-16.0	3.0	71.8	143.0	170.0	358.7
25	HSE06	-506.0	-354.2	-54.2	-16.7	3.2	71.4	142.7	169.2	360.5
27	M06	-632.0	-436.0	-71.8	-28.0	3.0	137.9	229.5	294.0	385.8
40.15	SOGGA	-284.3	-220.4	-26.4	-9.8	1.1	58.8	108.6	128.8	348.5
50	BHandHLYP	-160.2	-132.0	-12.4	-5.3	0.7	45.6	80.4	91.0	349.3
54	M06-2X	-177.0	-143.0	-13.0	-6.0	0.8	29.8	65.1	75.0	285.0
100	M06-HF	-64.0	-44.0	-1.0	-1.0	0.2	-7.3	12.3	11.0	147.7
	EXP	-382.0	-286.0	-39.7	-19.0	2.5	29.0	38.0	111.0	230.0
0-100	ω B97XD	-391.0	-296.0	-40.1	-14.4	1.6	68.4	142.7	170.4	371.1
0-100	CAM-B3LYP	-392.5	-291.9	-39.9	-13.9	1.7	68.3	136.8	161.8	390.2
0-100	LC- ω PBE	-497.9	-271.3	-36.3	-14.1	1.5	57.8	130.9	153.7	464.9
42.8-100	M11	-221.1	-167.3	-16.8	-8.6	0.3	43.7	82.5	100.9	354.5
25-25	PBE0	-492.0	-346.0	-51.6	-16.0	3.0	71.8	143.0	170.0	358.7
25	HSE06	-506.0	-354.2	-54.2	-16.7	3.2	71.4	142.7	169.2	360.5
25-0	N12SX	-462.3	-324.8	-48.7	-17.5	1.4	36.4	111.7	132.4	446.0
25-0	MN12SX	-497.4	-365.4	-47.7	-15.0	1.5	51.0	146.1	183.0	279.7

Table 3. Relative deviation (in %) of calculated DFT J values with respect to the experiment of the selected global hybrid DFT functionals. Color code: green (0-25 %), yellow (25-50 %), green (50-75 %), pink (75-100 %) and red (>100 %). Values in blue indicate overestimation with respect the experimental value with sign.

HF %	Functional	BISDOW	CUAQAC02	QAQVIP	CAVXUS	XAMBUI	PATFOG	JEJCIK	YAFZOU	LIZVOF
0	M06-L	-245	-163	-249	-32	820	313	620	201	-39
10	TPSSh	-141	-105	-165	-41	253	81	356	74	-1
20	B3LYP	-66	-50	-79	-12	56	158	330	74	32
21,8	X3LYP	-51	-39	-60	-1	40	158	314	68	40
22,95	APFD	-43	-32	-48	4	34	155	298	62	50
25	PBE0	-29	-21	-30	16	20	148	276	53	56
40,15	SOGGA	26	23	34	48	-54	103	186	16	52
50	BHandHLYP	58	54	69	72	-72	57	112	-18	52
54	M06-2X	54	50	67	68	-68	3	71	-32	24
100	M06-HF	83	85	97	95	-92	-125	-68	-90	-36

Table 4. Relative deviation (in %) of calculated DFT J values with respect to the experiment of the selected range separated hybrid DFT functionals. The HF % fraction in the short and long ranges of the exchange functional (S-L %HF) is indicated for each functional. The PBE0 global hybrid is included for comparison to complete the transition between short range and long range correction schemes. Color code: green (0-25 %), yellow (25-50 %), green (50-75 %), pink (75-100 %) and red (>100 %). Values in blue indicate overestimation with respect the experimental value with sign.

S-L HF %	Functional	BISDOW	CUAQAC02	QAQVIP	CAVXUS	XAMBUI	PATFOG	JEJCIK	YAFZOU	LIZVOF
0-100	ω B97XD	-2	-4	-1	24	-36	136	275	54	61
0-100	CAM-B3LYP	-3	-2	-1	27	-30	135	260	46	70
0-100	LC- ω PBE	-30	5	9	26	-39	99	244	38	102
42,8-100	M11	42	42	58	55	-86	51	117	-9	54
25-25	PBE0	-29	-21	-30	16	20	148	276	53	56
25-0	HSE06	-32	-24	-37	12	29	146	276	52	57
25-0	N12SX	-21	-14	-23	8	-44	26	194	19	94
25-0	MN12SX	-30	-28	-20	21	-40	76	285	65	22

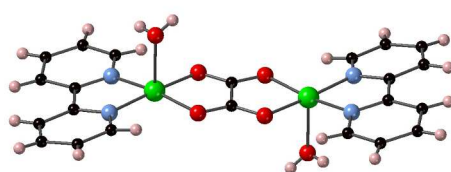
Table 5. Mean absolute error (MAE) values for J_{calc} with respect to J_{expt} (in cm^{-1}) using global hybrid DFT functionals. Different ranges of J values are explored.

HF %	Functional	(ALL)	(AF)	(FM)	$-40 < J < 30 \text{ cm}^{-1}$
0	M06-L	241	376	132	54
10	TPSSh	129	228	50	26
20	B3LYP	84	107	66	20
21,8	X3LYP	74	83	67	18
22,95	APFD	69	69	69	16
25	PBE0	58	46	67	15
27	M06	120	110	128	131
40,15	SOGGA	47	46	48	15
50	BHandHLYP	69	104	40	38
54	M06-2X	56	97	24	13
100	M06-HF	96	154	49	15

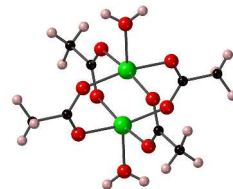
Table 6. Mean absolute error (MAE) values for J_{calc} with respect to J_{expt} (in cm^{-1}) using range separated hybrid DFT functionals. Different ranges of J values are explored and the PBE0 global hybrid is included for comparison.

HF %	Functional	(ALL)	(AF)	(FM)	$-40 < J < 30 \text{ cm}^{-1}$
0-100	ω B97XD	41	6	69	11
0-100	CAM-B3LYP	41	5	70	11
0-100	LC- ω PBE	60	35	80	10
42,8-100	M11	57	78	39	13
25-25	PBE0	58	46	67	15
25-0	HSE06	61	52	67	15
25-0	N12SX	50	32	51	5
25-0	MN12SX	51	52	64	9

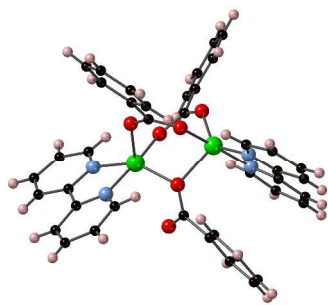
Figure 1. Molecular and ionic fragments of compounds 1-9 studied in the present work



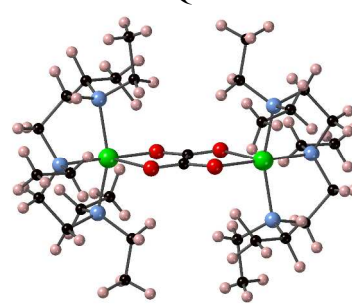
BISDOW



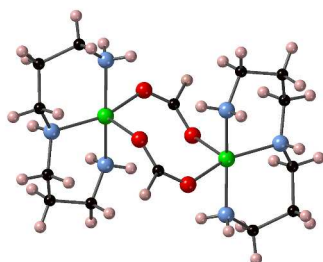
CUAQAC02



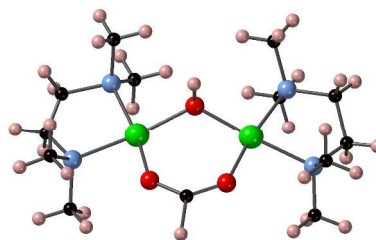
QAQVIP



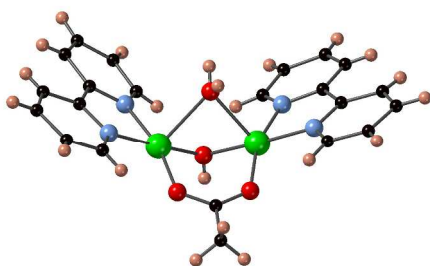
CAVXUS



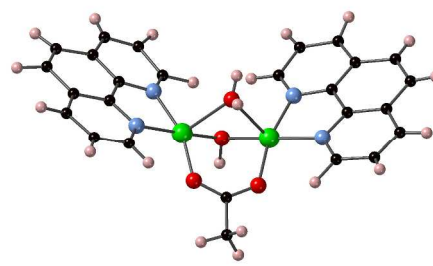
XAMBUI



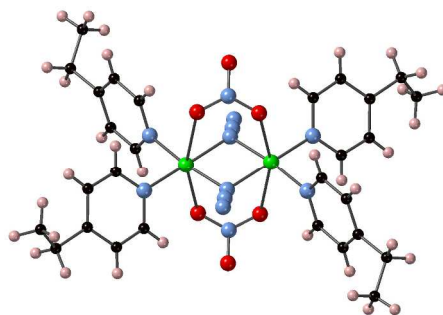
PATFOG



JEJCIK



YAFZOU



LIZVOF

Figure 2. Magnetic coupling constant of the compounds studied in the present work as predicted by the different exchange correlation functionals. The continuous line correspond to the experimental values.

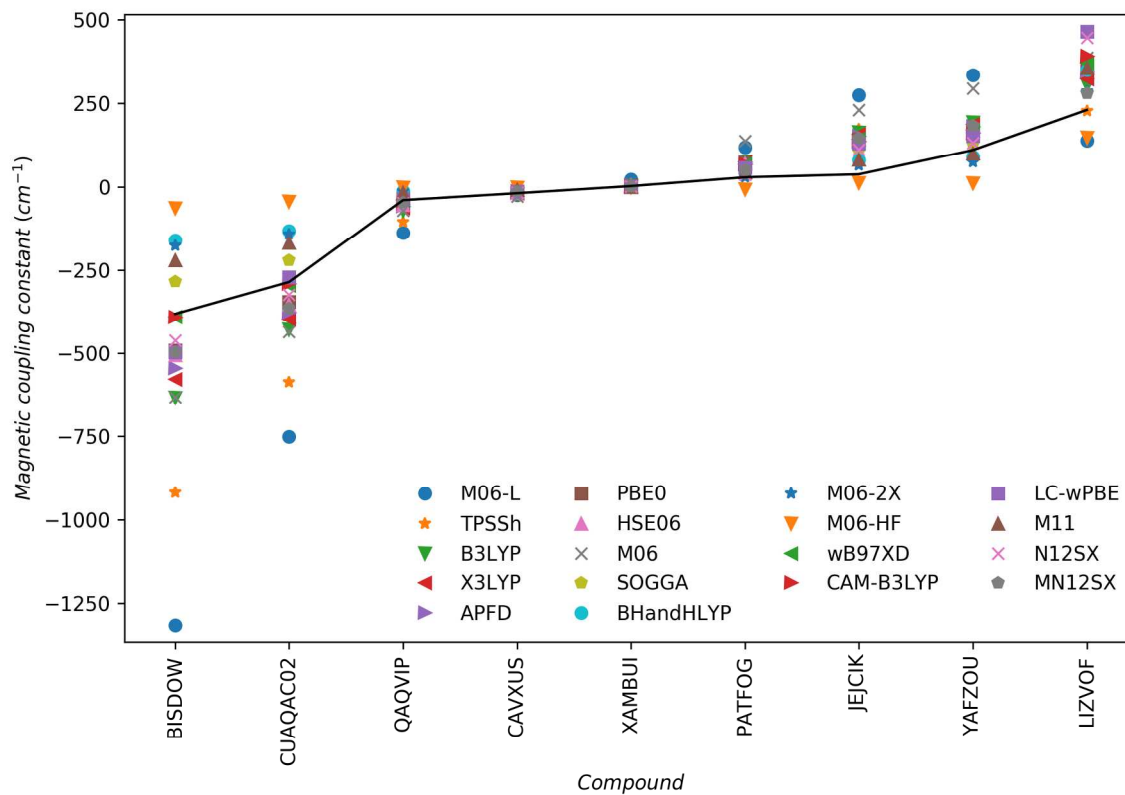
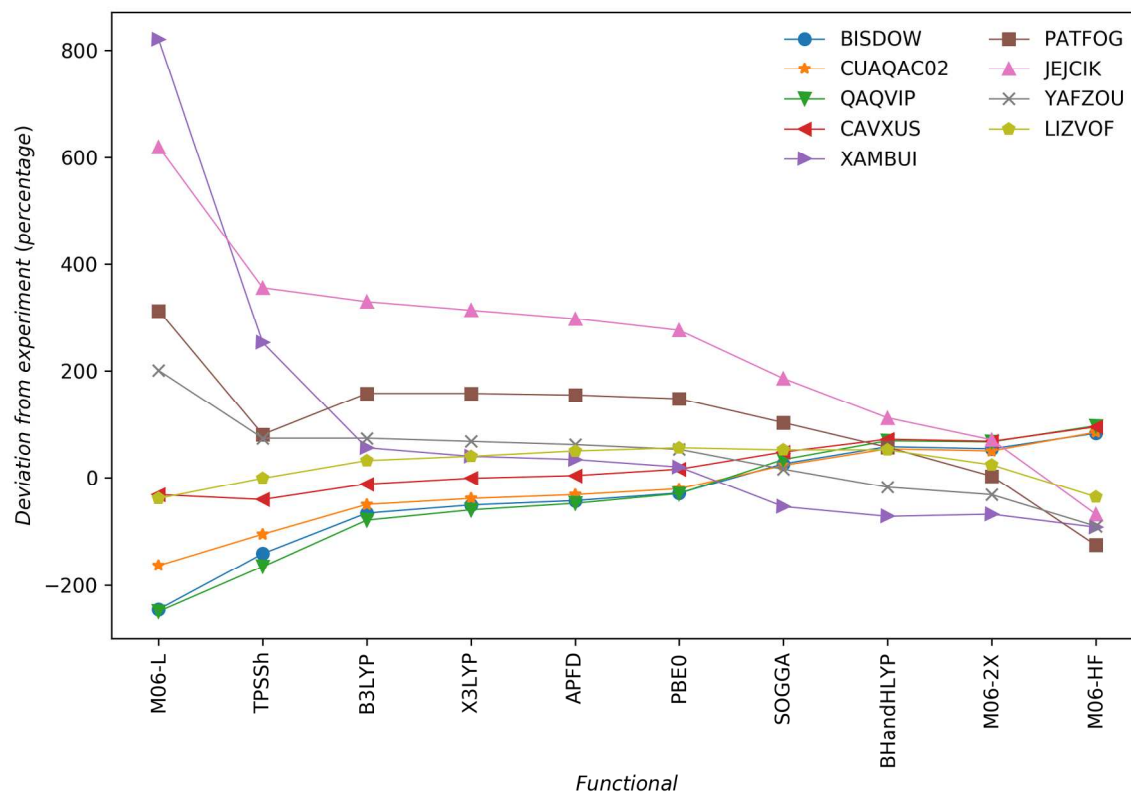


Figure 3. For each of the compounds on the data base, deviation from experiment of values calculated with each different DFT based method.



References

- ¹ Garrod C.; Percus, J.K. Reduction of N-Particle Variational Problem. *J. Math. Phys.* **1964**, *5*, 1756.
- ² McWeeny, R. *Methods of Molecular Quantum Mechanics*, 2nd ed. (Academic Press, Oxford, 1992).
- ³ Caballero, M.; Moreira, I. de P. R.; Bofill, J. M. A Comparison Model between Density Functional and Wave Function Theories by means of the Lowdin Partitioning Technique. *J. Chem. Phys.* **2013**, *138*, 174107.
- ⁴ Hohenberg, P.; Kohn, W. Inhomogeneous Electron Gas. *Phys. Rev.* **1964**, *136*, B864-B871.
- ⁵ Kohn, W.; Sham, L. J. Self-Consistent Equations Including Exchange and Correlation Effects. *Phys. Rev.* **1965**, *140*, A1133-A1138.
- ⁶ Parr, R.G.; Yang, W. in *Density-Functional Theory of Atoms and Molecules*, Oxford University Press, New York, **1989**.
- ⁷ Jones, R. O. Density Functional Theory: Its Origins, Rise to Prominence, and Future. *Rev. Mod. Phys.* **2015**, *87*, 897-923.
- ⁸ Medvedev, M. G.; Bushmarinov, I. S.; Sun, J.; Perdew, J. P.; Lyssenko, K. A. Density Functional Theory is Straying from the Path Toward the Exact Functional. *Science* **2017**, *355*, 49-52.
- ⁹ Wang, Y.; Wang, X. W.; Truhlar, D. G.; He, X. How Well Can the M06 Suite of Functionals Describe the Electron Densities of Ne, Ne⁶⁺, and Ne⁸⁺?. *J. Chem. Theory Comput.* **2017**, *13*, 6068-6077.
- ¹⁰ Ranasinghe, D. S.; Perera, A.; Bartlett, R. J. A note on the accuracy of KS-DFT densities. *J. Chem. Phys.* **2017**, *147*, 204103.
- ¹¹ Mezei, P. D.; Csonka, G. I.; Kallay, M. Electron Density Errors and Density-Driven Exchange-Correlation Energy Errors in Approximate Density Functional Calculations. *J. Chem. Theory Comput.* **2017**, *13*, 4753-4764.
- ¹² Valero, R.; Costa, R.; Moreira, I. de P. R.; Truhlar, D. G.; Illas, F. Performance of the M06 Family of Exchange-Correlation Functionals for Predicting Magnetic Coupling in Organic and Inorganic Molecules. *J. Chem. Phys.* **2008**, *128*, 114103.

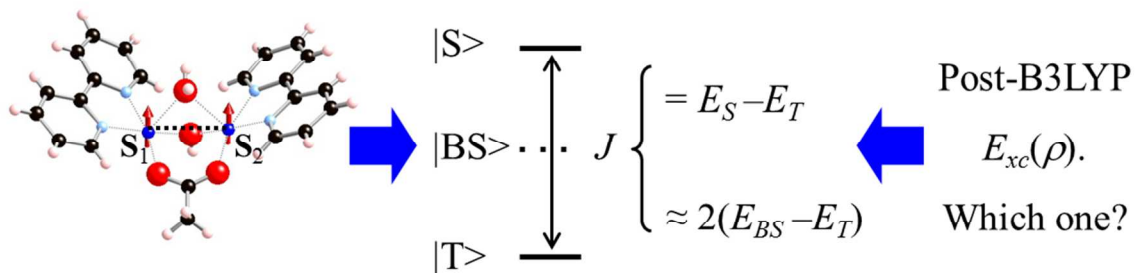
- 1
2
3
4 13 Rivero, P.; Moreira, I. de P. R.; Illas, F.; Scuseria, G. E. Reliability of Range Separated
5 Hybrids Functionals in Describing Magnetic Coupling in Molecular Systems. *J. Chem.*
6 *Phys.* **2008**, *129*, 184110.
7
8
9 14 <http://www.ccdc.cam.ac.uk/products/csd/>. The crystal structure data were downloaded in
10 CIF format from the CCDC database with the help of the ConQuest utility.
11
12 15 Castillo, O.; Muga, I.; Luque, A.; Gutierrez-Zorrilla, J.M.; Sertucha, J.; Vitoria, P.;
13 Roman, P. Synthesis, Chemical Characterization, X-Ray Crystal Structure and Magnetic
14 Properties of Oxalato-Bridged Copper(II) Binuclear Complexes with 2,2'-Bipyridine
15 and Diethylenetriamine as Peripheral Ligands. *Polyhedron* **1999**, *18*, 1235-1245.
16
17 16 de Meester, P.; Fletcher, S.R.; Skapski, A.C. Refined Crystal-Structure of Tetra-Mu-
18 Acetato-Bis-aquodocopper(II). *J. Chem. Soc., Dalton Trans.* **1973**, 2575-2578.
19
20 17 Sletten, J. The Structures of 2 Oxalato-Bridged Cu-Dimers -
21 [Cu₂(Me₄En)₂(C₂O₄)(H₂O)₂](PF₆)₂ · 2H₂O and [Cu₂(Et₅Dien)₂(C₂O₄)](PF₆)₂. *Acta Chem.*
22 *Scand. A* **1983**, *37*, 569-578.
23
24 18 Lopez, C.; Costa, R.; Illas, F.; Molins E.; Espinosa, E. The First Ferromagnetic Copper
25 (II) Complex Containing Ferrocenecarboxylato Bridging Ligands. *Inorg. Chem.* **2000**,
26 *39*, 4560-4565.
27
28 19 Tokii, T.; Hamamura, N.; Nakashima, M.; Muto, Y. Crystal-Structures and Magnetic-
29 Properties of Novel Mu-Carboxylato-Mu-Hydroxo-Bridged Binuclear Copper(II)
30 Complexes with 1,10-Phenanthroline. *Bull. Chem. Soc. Jpn.* **1992**, *65*, 1214-1219.
31
32 20 Wannarit, N.; Siriwong, K.; Chaichit, N.; Youngme, S.; Costa, R.; Moreira, I. de P.R.;
33 Illas, F. A New Series of Triply-Bridged Dinuclear Cu(II) Compounds: Synthesis,
34 Crystal Structure, Magnetic Properties and Theoretical Study. *Inorg. Chem.* **2011**, *50*,
35 10648-10659.
36
37 21 Lopez, C.; Costa, R.; Illas, F.; de Graaf, C.; Turnbull, M.; Landee, C.P.; Espinosa, E.;
38 Mata, I.; Molins E. Magnetostructural Correlations in Binuclear Copper(II) Compounds
39 Bridged, a Ferrocenecarboxylato(-1) and an Hydroxo- or Methoxo- Ligands: Tuning the
40 Sign of Superexchange in Heterobridged Complexes. *Dalton Trans.* **2005**, 2322-2330.
41
42 22 Christou, G.; Perlepes, S.P.; Folting, K.; Huffman, J.C.; Webb, R.J.; Hendrickson, D.N.
43 A New Class of Bipyridine-Ligated Metal Carboxylate Complexes - Characterization of
44
45
46
47
48
49
50
51
52
53
54
55
56
57
58
59
60

- 1
2
3
4 The Triply-Bridged Ferromagnetically-Coupled Complexes $[\text{Cu}_2(\text{Oac})_3(\text{Bpy})_2](\text{ClO}_4)$
5 and $[\text{Cu}_2(\text{OH})(\text{H}_2\text{O})(\text{Oac})(\text{Bpy})_2](\text{ClO}_4)_2$. *Chem. Commun.* **1990**, 746-747.
- 6
7
8 ²³ Escuer, A.; Goher, M.A.S.; Mautner, F.A.; Vicente, R. Three New Polynuclear
9 Copper(II) Complexes with the Symmetric $[\text{Cu}(\mu_{1,1}\text{-N}_3)_2\text{Cu}]^{2+}$ Core and Pyridine
10 Derivatives: Syntheses, Structure, and Magnetic Behavior *Inorg. Chem.* **2000**, *39*, 2107-
11 2112.
- 12
13
14 ²⁴ Becke, A. D. Density-Functional Thermochemistry.3. The Role Of Exact Exchange. *J.*
15 *Chem. Phys.* **1993**, *98*, 5648-5652.
- 16
17
18 ²⁵ Lee, C.; Yang, W.; Parr, R. G. Development of the Colle-Salvetti Correlation-Energy
19 Formula into a Functional of the Electron-Density. *Phys Rev B* **1988**, *37*, 785-789.
- 20
21
22 ²⁶ Adamo, C.; Barone, V. Toward Reliable Density Functional Methods without
23 Adjustable Parameters: The PBE0 Model. *J. Chem. Phys.*, **110** (1999) 6158-6170.
- 24
25
26 ²⁷ Ernzerhof, M.; Scuseria, G. E. Assessment of the Perdew–Burke–Ernzerhof Exchange-
27 Correlation Functional. *J. Chem. Phys.*, 1999, **110**, 5029-5036
- 28
29
30 ²⁸ Becke, A. D. A New Mixing of Hartree–Fock and Local Density-Functional Theories. *J.*
31 *Chem. Phys.* **1993**, *98*, 1372-1377.
- 32
33
34 ²⁹ Tao, J. M.; Perdew, J. P.; Staroverov, V. N.; Scuseria, G. E. Climbing the Density
35 Functional Ladder: Nonempirical Meta-Generalized Gradient Approximation Designed
36 for Molecules and Solids. *Phys. Rev. Lett.* **2003**, *91*, 146401.
- 37
38
39 ³⁰ Staroverov, V. N.; Scuseria, G. E.; Tao, J. M.; Perdew, J. P. Comparative Assessment of
40 a New Nonempirical Density Functional: Molecules and Hydrogen-bonded Complexes.
41 *J. Chem. Phys.*, **2003**, *119*, 12129. *ibid.* **2004**, *121*, 11507(Erratum).
- 42
43
44 ³¹ Xu, X.; Goddard III, W. A. The X3LYP Extended Density Functional for Accurate
45 Descriptions of Nonbond Interactions, Spin States, and Thermochemical Properties.
46 *Proc. Natl. Acad. Sci. USA* **2004**, *101*, 2673-77.
- 47
48
49 ³² Austin, A.; Petersson, G. A.; Frisch, M. J.; Dobek, F. J.; Scalmani, G.; Throssell, K. A
50 Density Functional with Spherical Atom Dispersion Terms. *J. Chem. Theory Comput.*
51 **2012**, *8*, 4989-5007.
- 52
53
54 ³³ Zhao, Y.; Truhlar, D. G. The M06 Suite of Density Functionals for Main Group
55 Thermochemistry, Thermochemical Kinetics, Noncovalent Interactions, Excited States,
56
57
58
59
60

- and Transition Elements: Two New Functionals and Systematic Testing of Four M06-Class Functionals and 12 Other Functionals. *Theor. Chem. Acc.* **2008**, *120*, 215-241.
- ³⁴ Zhao, Y.; Truhlar, D. G. Comparative DFT Study of Van der Waals Complexes: Rare-Gas Dimers, Alkaline-Earth Dimers, Zinc Dimer, and Zinc-Rare-Gas Dimers. *J. Phys. Chem. A* **2006**, *110*, 5121-5129;
- ³⁵ Zhao, Y.; Truhlar, D. G. Density Functional for Spectroscopy: No Long-Range Self-Interaction Error, Good Performance for Rydberg and Charge-Transfer States, and Better Performance on Average than B3LYP for Ground States. *J. Phys. Chem. A* **2006**, *110*, 13126-13130.
- ³⁶ Zhao, Y.; Truhlar, D. G. A New Local Density Functional for Main-Group Thermochemistry, Transition Metal Bonding, Thermochemical Kinetics, and Noncovalent Interactions. *J. Chem. Phys.* **2006**, *125*, 194101.
- ³⁷ Peverati, R.; Truhlar, D. G. A Global Hybrid Generalized Gradient Approximation to the Exchange-Correlation Functional that Satisfies the Second-Order Density-Gradient Constraint and Has Broad Applicability in Chemistry. *J. Chem. Phys.* **2011**, *135*, 191102.
- ³⁸ Heyd, J.; Scuseria, G. E.; Ernzerhof, M. Hybrid Functionals Based on a Screened Coulomb Potential. *J. Chem. Phys.* **2003**, *118*, 8207-8215; *ibid.* **2006**, *124*, 219906 (E).
- ³⁹ Peverati, R.; Truhlar, D. G. Screened-Exchange Density Functionals with Broad Accuracy for Chemistry and Solid-State Physics. *Phys. Chem. Chem. Phys.* **2012**, *14*, 16187-16191.
- ⁴⁰ Chai, J.-D.; Head-Gordon, M. Long-Range Corrected Hybrid Density Functionals with Damped Atom-Atom Dispersion Corrections. *Phys. Chem. Chem. Phys.* **2008**, *10*, 6615-6620
- ⁴¹ Yanai, T.; Tew, D.; Handy, N. A New Hybrid Exchange-Correlation Functional Using the Coulomb-Attenuating Method (CAM-B3LYP). *Chem. Phys. Lett.* **2004**, *393*, 51-57.
- ⁴² Vydrov O. A.; Scuseria, G. E. Assessment of a Long-Range Corrected Hybrid Functional. *J. Chem. Phys.* **2006**, *125*, 234109.
- ⁴³ Vydrov, O. A.; Heyd, J.; Krukau, A. V.; Scuseria, G. E. Importance of Short-Range versus Long-Range Hartree-Fock Exchange for the Performance of Hybrid Density Functionals. *J. Chem. Phys.* **2006**, *125*, 074106.

- 1
2
3
4 44 Peverati, R.; Truhlar, D. G. Improving the Accuracy of Hybrid Meta-GGA Density
5 Functionals by Range Separation. *J. Phys. Chem. Lett.* **2011**, *2*, 2810-2817.
6
7
8 45 Moreira, I. de P. R.; Costa, R.; Filatov, M.; Illas, F. Restricted Ensemble-Referenced
9 Kohn Sham versus Broken Symmetry Approaches in Density Functional Theory:
10 Magnetic Coupling in Cu Binuclear Complexes. *J. Chem. Theory and Comput.* **2007**, *3*,
11 764-774.
12
13
14 46 Costa, R.; Moreira, I. de P.R.; Youngme, S.; Siriwong, K.; Wannarit, N.; Illas, F.
15 Towards the Design of Ferromagnetic Molecular Complexes: Magnetostructural
16 Correlations in Ferromagnetic Triply-Bridged Dinuclear Cu(II) Compounds Containing
17 Carboxylato and Hydroxo Bridges. *Inorg. Chem.* **2010**, *49*, 285-294.
18
19
20
21 47 Wannarit, N.; Pakawatchai, Ch.; Mutikainen, I.; Costa, R.; Moreira, I. de P. R.;
22 Youngme, S.; Illas, F. Hetero Triply-Bridged Dinuclear Copper(II) Compounds with
23 Ferromagnetic Coupling: A Challenge for Current Density Functionals. *Phys. Chem.*
24 *Chem. Phys.* **2013**, *15*, 1966-1975.
25
26
27
28 48 Muñoz, D.; de Graaf, C.; Illas, F. Putting Error Bars on the Ab Initio Theoretical
29 Estimates of the Magnetic Coupling Constants: The Parent Compounds of
30 Superconducting Cuprates as a Case Study. *J. Comput. Chem.* **2004**, *25*, 1234-1241
31
32
33 49 Frisch, M. J.; Trucks, G. W.; et al. *Gaussian 09*, Revision **A.1**; J. Gaussian, Inc.:
34 Wallingford CT, **2009**.
35
36
37
38
39
40
41
42
43
44
45
46
47
48
49
50
51
52
53
54
55
56
57
58
59
60

Graphic for TOC



The reliability of calculated J values using post-B3LYP functionals is system and range dependent.